ACADEMIC
PRESS

Available online at www.sciencedirect.com

SCIENCE DIRECT

Journal of Solid State Chemistry 171 (2003) 299–303

JOURNAL OF
SOLID STATE
CHEMISTRY

http://elsevier.com/locate/jssc

A simple model for $f \rightarrow d$ transitions of rare-earth ions in crystals

C.K. Duan and M.F. Reid*

Department of Physics and Astronomy, University of Canterbury, Private Bag 4800, Christchurch 8020, New Zealand

Received 6 May 2002; received in revised form 20 August 2002; accepted 23 August 2002

Abstract

Theoretical simulation and interpretation of $f \rightarrow d$ transitions of rare earth ions in crystals are more difficult than for $f \rightarrow f$ transitions, because $f \rightarrow d$ transitions involve many more energy levels and are further complicated by strong vibronic transitions, so the experimental spectra contain many fewer resolvable peaks. In order to better understand the structure of the spectra, a simple model is developed to take into account the main interactions in the $f^{N-1}d$ configuration. This model leads to quantum numbers characterizing the states and the associated transition selection rules. Relative transition intensities can be quantitatively estimated. The model is applied to Eu^{2+} and Sm^{3+} ions in crystals.

1. Introduction

It is well known that $f \rightarrow f$ spectra of rare-earth ions are characterized by many sharp lines. The energy levels are well resolved and the symmetry properties may be determined from polarized spectra. The energy level structure is characterized by weak splitting of the quasi-free-ion energy levels, which change little from host to host. Modeling of the experimental energy levels and transition probabilities with a crystal–field model Hamiltonian [1] and Judd–Ofelt theory [2,3] are well known.

In comparison, the $f \rightarrow d$ transitions are less well understood experimentally and theoretically, partly because the $f \rightarrow d$ transitions for trivalent rare-earth ions generally lie in the ultraviolet or vacuum ultraviolet region, making them experimentally less accessible. The divalent rare-earth ions have transitions of lower energy but the divalent oxidization states are usually unstable. Nevertheless, there have been some measurements on $f \rightarrow d$ transitions for Eu^{2+}, Sm^{2+} and Yb^{2+} in halide crystals, and more recently, for most trivalent ions in $LiYF_4$, CaF_2 and YPO_4 hosts. The $f \rightarrow d$ transitions are characterized by broad bands with very little structure, even though there are many energy levels involved in the $f \rightarrow d$ transitions. The structure of the $f \rightarrow d$ transition spectra are quite different for a particular ion in different hosts but in many cases there are similarities for different ions in the same host. Theoretical models have been proposed to explain $f \rightarrow d$ transitions of divalent ions in crystals. These models assumed that there is no interaction between the f^{N-1} core and the d electron. For example, Eu^{2+} in CaF_2 contains two broad bands in the UV region, with a "staircase" structure for the band with lower energy. The two broad bands were assigned to be transition [5] from the f^7 ground state to the f^6d states with the d electron in e_g and t_{2g} orbitals. The staircase was assigned to be the splitting of the ground states of f^6 core by spin–orbit interaction [5]. Later calculations showed that the Coulomb interaction of the f and d electrons cannot be assumed to be small [7]. Full energy level and transition intensity calculations that include all the bases and interactions for the f^N and $f^{N-1}d$ configurations are now possible. Extensive calculations have been carried out for trivalent rare-earth ions in crystals [9,10]. These calculations are similar to those for f^N but require many more physical parameters as input: the energy level parameters for the f^N configuration and for the f^{N-1} core of the $f^{N-1}d$ configuration, the crystal–field parameters for d electron, and the parameters describing the Coulomb interaction between f electrons and the d electron. There is no adjustable parameter for the relative intensities of the dipole-allowed transitions, but a model to describe the vibronic profile is essential and this has been simplified with three adjustable parameters: the offset and the bandwidth of the vibronic band and the

---

*Corresponding author. Fax: +64-3-364-2469.
E-mail address: M.reid@phys.canterbury.ac.nz (M.F. Reid).

0022-4596/03/$ - see front matter © 2003 Published by Elsevier Science (USA).
doi:10.1016/S0022-4596(02)00181-0

intensity ratio of the zero-phonon line to the vibronic band. These calculations gave satisfactory agreement with the experiments.

The $f \to f$ spectra, containing plentiful fine structure, have been understood both qualitatively and quantitatively with a simple crystal–field Hamiltonian and Judd–Ofelt theory with adjustable parameters. However, the $f \to d$ spectra, in which fewer peaks are resolved, have required more complicated calculations and the interpretation of the results of these calculations are quite difficult. Here, we develop a simple model to understand the $f \to d$ transitions qualitatively. The model uses two quantum numbers to characterize the energy levels. These quantum numbers may be used to derive selection rules and relative transition intensities can be estimated based on the approximate wavefunctions. The model is applied to Eu^{2+} and Sm^{3+} ions in crystals to give a qualitative explanation of the experimental results.

2. Model

2.1. Model Hamiltonian for the $f^{N-1}d$ configuration and general energy level structure

The Hamiltonian for the $f^{N-1}d$ configuration can be written as

$$H = H_{\mathrm{Coul}}(ff) + H_{\mathrm{so}}(f) + H_{\mathrm{c}}(f) + H_{\mathrm{c}}(d) + H_{\mathrm{so}}(d) + H_{\mathrm{Coul}}(fd), \tag{1}$$

where the subscript "Coul", "so" and "c" represent Coulomb interaction, spin–orbit interaction and crystal–field interaction, respectively, and "f" and "d" are the electrons involved in the interactions.

The strongest interactions are the Coulomb interaction between f electrons and the crystal–field interaction for the d electron. The former splits f^{N-1} into energy levels characterized by quantum numbers for the spin, S_f, and the orbital angular momentum, L_f. These energy levels are denoted as $|\eta S_f L_f\rangle$, where η is a multiplicity number to distinguish different levels with the same S_f and L_f. The latter splits d into crystal field energy levels $|{}^2d_i\rangle$. These splittings are in the order of magnitude of $10^4\ \mathrm{cm}^{-1}$. We shall write these two interactions as

$$H_0 = H_{\mathrm{Coul}}(ff) + H_{\mathrm{c}}(d). \tag{2}$$

The eigenstates of H_0 can then be written as $|\eta S_f L_f, {}^2d_i\rangle$.

These energy levels are further split by the isotropic exchange part of $H_{\mathrm{Coul}}(fd)$ into high-spin and low-spin sets separated by a few thousand wave numbers. There are also splittings in each set due to the other part of $H_{\mathrm{Coul}}(fd)$ and will be neglected in the following analysis. The part of $H_{\mathrm{Coul}}(fd)$ that contributes to the splitting between high- and low-spin states can be written as an exchange Hamiltonian

$$H_{\mathrm{ex}}(fd) = -J_{\mathrm{ex}} \mathbf{S}_f \cdot \mathbf{s}_d, \tag{3}$$

where J_{ex} is a function of $|\eta S_f L_f, {}^2d_i\rangle$. Its value can be estimated from the average exchange interaction strength between f and d electrons, i.e.,

$$J_{\mathrm{ex}} = \frac{6}{35} G_1(fd) + \frac{8}{105} G_3(fd) + \frac{20}{231} G_5(fd), \tag{4}$$

where $G_{1,3,5}(fd)$ are f–d Coulomb exchange radial integrals. $H_{\mathrm{ex}}(fd)$ commutes with the total spin operator

$$\mathbf{S} = \mathbf{S}_f + \mathbf{s}_d. \tag{5}$$

The energy levels for H_{ex} can be written as $|(\eta S_f L_f, {}^2d_i)S\rangle$, where S is the quantum number of the total spin $\mathbf{S}$.

The next-largest interactions are the spin–orbit interactions $H_{\mathrm{so}}(f)$ and $H_{\mathrm{so}}(d)$, which have an order of magnitude of $1000\ \mathrm{cm}^{-1}$. In low-degeneracy cases it is not necessary to consider $H_{\mathrm{so}}(d)$ as the orbital angular momentum of the d electron is quenched in the sense that $H_{\mathrm{so}}(d)$ only shifts the crystal–field states by a small amount. In the few high-degeneracy cases, such as the t_{2g} type d orbital in a site with O_h symmetry, $H_{\mathrm{so}}(d)$ splits the t_{2g} states and needs to be considered. We shall consider the low-degeneracy cases only and neglect $H_{\mathrm{so}}(d)$ for simplicity. The splitting caused by $H_{\mathrm{c}}(f)$ has an order of magnitude of $100\ \mathrm{cm}^{-1}$, the same order of magnitude as optical phonon energies. This cannot usually be well-resolved experimentally. We shall consider $H_{\mathrm{so}}(f)$ only and neglect the other weak interactions. $H_{\mathrm{so}}(f)$ commutes with the following "angular momentum" operator:

$$\mathbf{J} = \mathbf{S}_f + \mathbf{s}_d + \mathbf{L}_f. \tag{6}$$

This operator is different from the total angular momentum operator for $f^{N-1}d$ in that it does not contains the orbital angular momentum for d, which can usually be considered to be quenched.

The interaction $H_{\mathrm{so}}(f)$ splits the $|(\eta S_f L_f, {}^2d_i)S\rangle$ into several energy levels characterized by the quantum number J, which can be denoted as $|(\eta S_f L_f, {}^2d_i)SJ\rangle$. Apart from this splitting, there is also small mixing by $H_{\mathrm{so}}(f)$ of $|(\eta S_f L_f, {}^2d_i)SJ\rangle$ with bases of the same J but different S_f, L_f and S, which may be important for spin-forbidden transitions. We shall neglect this mixing when considering spin-allowed transitions.

With these simplifications, we can write the model Hamiltonian as

$$H_{\mathrm{eff}} = H_0 - J_{\mathrm{ex}} \mathbf{S}_f \cdot \mathbf{S}_d + \lambda_{S,L_f} \mathbf{S} \cdot \mathbf{L}_f, \tag{7}$$

where λ_{S,L_f} can be written in terms of the spin–orbit interaction parameter ξ_{4f}. It can be related to $\lambda_{\eta S_f L_f}$ [1] by

$$\lambda_{S,L_f} = \left(2 - \frac{2S+1}{2S_f+1}\right) \lambda_{\eta S_f L_f}. \tag{8}$$

In the case that S_f takes the largest possible value for the f^{N-1} configuration, $\lambda_{\eta S_f L_f}$ is simply $\mathrm{sign}(8-N)\xi_{4f}/2S_f$, and

$$\lambda_{S,L_f} = \mathrm{sign}(8-N)\left(2-\frac{2S+1}{2S_f+1}\right)\frac{\xi_{4f}}{2S_f}. \tag{9}$$

The eigenvectors and the corresponding eigenvalues can be written as $|(\eta S_f L_f, {}^2d_i)SJ\rangle$ and

$$\begin{aligned} E(\eta S_f L_f, {}^2d_i, SJ) &= E_0(\eta S_f L_f, {}^2d_i) \\ &- J_{\mathrm{ex}}[S(S+1) - S_f(S_f+1) - S_d(S_d+1)]/2 \\ &+ \lambda_{S,L_f}[J(J+1) - S(S+1) - L_f(L_f+1)]/2. \end{aligned} \tag{10}$$

2.2. *Selection rules and relative line strength for $f \to d$ transitions*

The f^N to $f^{N-1}d$ transitions are electric dipole allowed and so other mechanisms are negligible. The electric dipole moment D is a spin-independent rank 1 tensor in both total orbital angular momentum and total angular momentum spaces. It can be thought of as the coupling of the creation operator of an f electron (a rank $(\frac{1}{2},3)$ double tensor) to the annihilation operator of a d electron (a rank $(\frac{1}{2},2)$ double tensor). Using the angular momentum coupling scheme for $f^{N-1}d$ energy levels used above, i.e., $((S_f s_d)SL_f)J$ coupling, the m component of D can be expanded as

$$D_m = D_m^{(((\frac{1}{2}\cdot\frac{1}{2})0\cdot 3)3\cdot 2)1} = D^{3\cdot 2}_{m_J\cdot m_d}\langle 3m_J 2m_d|1m\rangle, \tag{11}$$

where m and m_J and m_d are labels to distinguish the partners of total angular momentum (rank 1), the quantum number for the angular momentum **J** (rank 3) and that for the d-electron orbital angular momentum (rank 2). $\langle 3m_J 2m_d|1m\rangle$ is a vector coupling coefficient.

The f^N energy levels $|\eta SLJ\rangle$ can also be put into $((S_f s_d)SL_f)J$ coupling form as $(\eta SL, {}^1 0)SJ\rangle$, where the d-electron spin and orbital angular momentum are zero as there is no d electron in f^N.

The transition between f^N energy level $|\eta SLJ\rangle$ and $f^{N-1}d$ energy level $(\eta' S_f L_f, {}^2d_i)S'J'\rangle$ must satisfy the selection rules

$$S = S', \tag{12}$$

$$|J-J'| \leqslant 3 \leqslant J+J'. \tag{13}$$

The relative line strengths for the electric dipole transitions that obey these selection rules can be calculated as

$$\begin{aligned} &I_m(|\eta SLJ\rangle \leftrightarrow |(\eta' S_f L_f, {}^2d_i)SJ'\rangle) \\ &= \sum_{m_J, m'_J m_{d_i}} |\langle \eta SLJm_J|D_m|(\eta' S_f L_f, {}^2d_i)SJ'm'_J m_{d_i}\rangle|^2 \\ &= \frac{(2J+1)(2J'+1)}{35(2S+1)}|\langle S\cdot L\cdot 0||D^{0\cdot 3\cdot 2}||S\cdot L_f\cdot 2\rangle|^2 \end{aligned} \tag{14}$$

$$\times \begin{Bmatrix} L & L_f & 3 \\ J' & J & S \end{Bmatrix}^2 \sum_{m_3, m_{d_i}} |\langle 3m_3, 2d_i m_{d_i}|1m\rangle|^2, \tag{15}$$

where $\langle S\cdot L\cdot 0||D^{0\cdot 3\cdot 2}||S\cdot L_f\cdot 2\rangle$ is a reduced matrix element that can be calculated from "coefficient of fractional parentage" for f^N and d states. The line strength for transitions involving isotropic light is

$$\begin{aligned} I_{\mathrm{iso}} &= \frac{(2J+1)(2J'+1)|d_i|}{175(2S+1)}\begin{Bmatrix} L & L_f & 3 \\ J' & J & S \end{Bmatrix}^2 \\ &\quad \times |\langle S\cdot L\cdot 0||D^{0\cdot 3\cdot 2}||S\cdot L_f\cdot 2\rangle|^2. \end{aligned} \tag{16}$$

The relative line strength for transitions from the same initial energy level to final energy levels differ only in the quantum number for **J** can be calculated without calculating the reduced matrix element.

3. Application to $f \to d$ transitions for Eu^{2+} and Sm^{3+} ions in crystals

We now give examples of a divalent and a trivalent rare-earth ion in crystals. These ions in the middle of the lanthanide series have thousands of energy levels and the full calculations [9,10] are hard to interpret, while those ions at the beginning and end of the lanthanide series have fewer energy levels and are much simpler. We shall choose Eu^{2+} (f^7) and Sm^{3+} (f^5) ions in crystals as examples.

3.1. Eu^{2+} *in alkaline-earth fluorides*

The $f \to d$ absorption spectra of Eu^{2+} have been studied by many authors [4–6]. The spectra contain two broad bands around 27,000 and 43,000 cm^{-1}. The low-energy band has a staircase structure of about seven peaks, with intensity increasing from low energy to high energy (see Figs. 2 and 3 of Ref. [6]). These peaks have been assigned to the seven ${}^7F_J$ ($J = 0, \ldots, 6$) multiplets of the f^6 core [5]. However, it was pointed out by Weakliem [7] that the *fd* Coulomb interaction cannot be considered to be weaker than spin–orbit interactions. Weakliem's calculation (Fig. 1 of Ref. [7]) shows that the ${}^7F$ multiplet of f^7 couples with ${}^2e_g$ and splits into a set of high-spin states and a set of low-spin states. Each set of states are split further by the spin–orbit interaction. According to our model, these states can be grouped in seven sets of octet states $|({}^7F, {}^2e_g)^8F'_J\rangle$ ($J' = 1/2, \ldots, 13/2$) and six sets of sextet states $|({}^7F, {}^2e_g)^6F'_J\rangle$ ($J' = 1/2, \ldots, 11/2$). The center position of each group can be estimated from Eq. (10) by using $J_{\mathrm{ex}} \approx 1500$ cm^{-1}, estimated from the $G_{1,3,5}$ value and $\lambda_{{}^7F} = 250$ cm^{-1} [7]. The ground-state absorption to these octet states obey both spin and "angular momentum" **J** selection rules. The relative line strengths

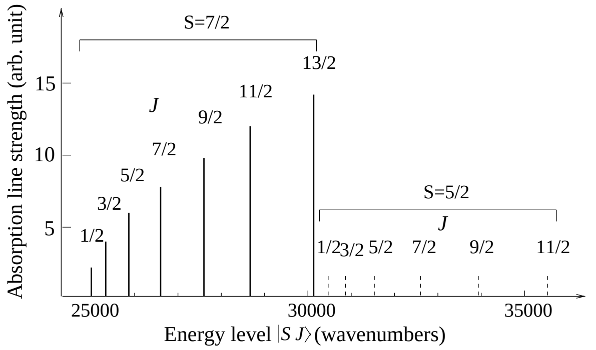

Fig. 1. Schematic diagram for the positions of $f \rightarrow d$ transition peaks and line strengths of the low-energy band of Eu^{2+} in CaF_2. Note that the line strengths for the spin-forbidden transitions are not calculated and the dashed lines represent only the positions.

can be easily estimated from Eqs. (15) and (16) by noticing that for this particular case every factor except $(2J' + 1)$ is constant. Therefore, the relative line strength is $(2J' + 1)$ for $|(^7F, ^2e_g)^8F'_J\rangle$ $(J' = 1/2, \ldots, 13/2)$. A schematic diagram for the energy levels and absorption line strengths is given in Fig. 1. This diagram reproduces the staircase structure of the low-energy band of the absorption spectra (note that since we use pure SL coupling for $4f^{N-1}$ states, there is a discrepancy of a few hundred wavenumbers between the estimated and measured peak positions). For the high-energy t_2 band, as it is not a low-degeneracy case, the orbital angular momentum of the d electron is not completely quenched and needs to be taken into account, making the analyses a little more complicated. However, the broadening due to relaxation to the conduction band hides the fine structure and makes these analyses unnecessary. The relative line strengths for the spin-forbidden transitions can also be estimated if the mixing due to the spin–orbit interaction is taken into account. They are much weaker than these spin-allowed transitions.

3.2. Sm^{3+} in YPO_4, CaF_2 and $LiYF_4$ crystals

The $f \rightarrow d$ absorption spectra for most trivalent rare-earth ions in YPO_4, CaF_2 and $LiYF_4$ crystals have been studied by van Pieterson et al. [8–11]. We choose Sm^{3+} as an example. The ground multiplet for Sm^{3+} (f^5) is $^6H_{5/2}$. The lowest sextet multiplets for f^4d are $|(^5I, ^2d_i)^6I_J\rangle$ $(J = 7/2, \ldots, 17/2)$ for each d crystal–field energy level ^2d_i. The splitting can be estimated using Eq. (10). The multiplets with $J = 7/2$, $9/2$ and $11/2$ are the only states to which the absorptions obey the $\Delta J \leqslant 3$ selection rule. The relative line strengths can be calculated from Eqs. (15) and (16) by noticing that every factor except $(2J' + 1)$ and the $6j$ symbol are constant. The intensity ratios are 144:125:18. The schematic diagram of energy level positions and relative intensities are given in Fig. 2. In all the experimental spectra of the three crystals, the first two peaks for the first d crystal–field energy level (peak A_1 and A_2 in Figs. 17–19 of Ref. [9]) have almost the same intensities and the third peak is almost an order of magnitude weaker. This agrees with our calculations. There is an additional very weak peak for the first d crystal–field energy level in CaF_2 and $LiYF_4$ corresponding to the transition to $|(^5I, ^2d_i)^6I_{13/2}\rangle$, which is forbidden by the ΔJ selection rule. This is probably due to J-mixing in either the ground multiplets or excited multiplets or both. The separation of these peaks in the experimental spectra are similar for all the three crystals and can be estimated by setting $\xi_{4f} \approx 1500\ \text{cm}^{-1}$. The model also predicts that such structure should repeat for each of the $5d$ crystal–field levels. However, the $5d$ crystal–field levels with higher energy are usually broadened by relaxation to the conduction band, or other relaxation mechanisms, and the structure is not well resolved. Nevertheless, in $LiYF_4$ the second $5d$ crystal–field level is well resolved [9]. It contains three peaks with separations and relative intensities agreeing with our prediction.

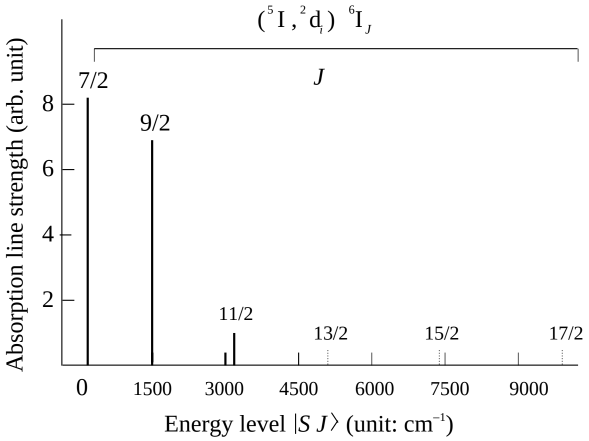

Fig. 2. Schematic diagram for the relative positions of $f \rightarrow d$ transition peaks (estimated with $\xi_{4f} = 1500\ \text{cm}^{-1}$) and line strengths of the band $(^5I, ^2d_i)$ of Sm^{3+} in the three crystals. Note that the line strengths for the **J**-forbidden transitions are not calculated and the dashed lines represent only the positions.

4. Conclusion

A simple model for $f \rightarrow d$ transitions that takes account of the main interactions in the $f^{N-1}d$ configuration is developed. This model leads to quantum numbers grouping the numerous $f^{N-1}d$ states. Selection rules and relative transition intensities are obtained based on these quantum numbers. This model is applied to Eu^{2+} and Sm^{3+} ions in various crystals and explains the experimental results.

References

[1] B.G. Wybourne, Spectroscopic Properties of Rare Earths, Interscience, New York, 1965 (Chapter 6).
[2] B.R. Judd, Phys. Rev. 127 (1962) 750.
[3] G.S. Ofelt, J. Chem. Phys. 37 (1962) 511.
[4] A.A. Kaplyanskii, P.P. Zakharchenya, Opt. Spektroskopiya 13 (1962) 597.
[5] E. Loh, Phys. Rev. 175 (1968) 533.
[6] C. Dujardin, B. Moine, C. Pedrini, J. Lumin. 54 (1993) 259.
[7] H.A. Weakliem, Phys. Rev. B 6 (1972) 2743.
[8] L. van Pieterson, R.T. Wegh, A. Meijerink, M.F. Reid, J. Chem. Phys. 115 (2001) 9382.
[9] L. van Pieterson, M.F. Reid, R.T. Wegh, S. Soverna, A. Meijerink, Phys. Rev. B 65 (2002) 045113.
[10] L. van Pieterson, M.F. Reid, G.W. Burdick, A. Meijerink, Phys. Rev. B 65 (2002) 045114.
[11] L. van Pieterson, M.F. Reid, A. Meijerink, Phys. Rev. Lett. 88 (2002) 067405.